Design and Fabrication of Calibration Device for Scintillating Fibers of Tagger Microscope: For use in GlueX's QCD Experiment

Briere, Emily F.

2012 National Science Foundation – BioGRID REU Fellows
Department of Computer Science and Engineering
University of Connecticut, Storrs, CT 06269

Department of Mechanical Engineering, Duke University, Durham, NC 27708

emily.briere@duke.edu

Abstract. For decades, scientists have struggled to understand the chromo-electromagnetic field which confines quarks and gluons within the hadron. GlueX is a quantum chromodynamics experiment centered at Jefferson Lab, Virginia, whose mission is to better understand this gluonic field by exciting it, and mapping the spectrum of exotic hybrid mesons that it generates. The experiment uses coherent bremsstrahlung radiation to produce a 9 GeV linearly polarized photon beam from a 12 GeV electron beam. Due to their polarity, the photons in this beam act as virtual vector mesons, and when incident on a liquid hydrogen target are expected to form exotic hybrid mesons. These particles quickly decay into new particles (mostly hadrons) which are captured in a solenoid detector. The decays can then be reconstructed to understand the properties of the original exotic hybrid meson. Importantly, the post-bremsstrahlung degraded electrons are bent from the main beam into the tagger microscope where they strike an array of scintillating optical fibers. Given the correlation between momentum and radial bend, the Silicon Photomultiplier sensors attached to the optical fibers are able to determine the electron's, and thus the photon's, initial energy based on which fiber was hit. This method of "tagging" the photons is an essential aspect of the experiment described here, specifically by providing the initial energy of the photon which is used to reconstruct the exotic meson. It is therefore crucial that the tagger provide accurate data. This paper details the design and fabrication of a calibration device for the scintillating fibers of the tagger microscope. The mechanical structure hovers over the tagger microscope and moves horizontally between fiber bundles, using a green laser diode to direct light pulses into the fibers. This calibration method has been tested mechanically and via a Monte Carlo Matlab simulation, and has proven to be effective. Despite being a small aspect of the greater GlueX project, such a calibration device is vital to experimental accuracy.

Keywords: Exotic Hybrid Meson, Gluonic Field, Tagger Microscope, Calibration Device, Reflection, Refraction, Beam Polarization, Monte Carlo Simulation

1 Introduction

1.1 Quantum Chromodynamics

Declared one of the top ten physics mysteries of the century, the confinement of quarks and gluons within the hadron is an essential area of research with significant implications. Quarks, along with leptons, are the smallest known building blocks of our universe. There are six different "flavors" of quarks: up, charm, top, down strange, and bottom. These different flavors combine in nonets (groups of nine) to form particles and make up the world around us. Yet despite their ever-present nature, quarks have yet to be isolated. Quarks and anti-quarks exist only in bundles known as hadrons, bound tightly by the force-carrier particles gluons. Hadrons manifest in two forms: baryons and mesons. Baryons are composed of three quarks (qqq), for instance a proton comprises two ups and one down (uud) quark, while a neutron comprises two downs and one up quark (udd). Far more basic, a meson is composed of one quark and one antiquark ($q\bar{q}$) [1]. Both of these hadrons are depicted in Figure 1:

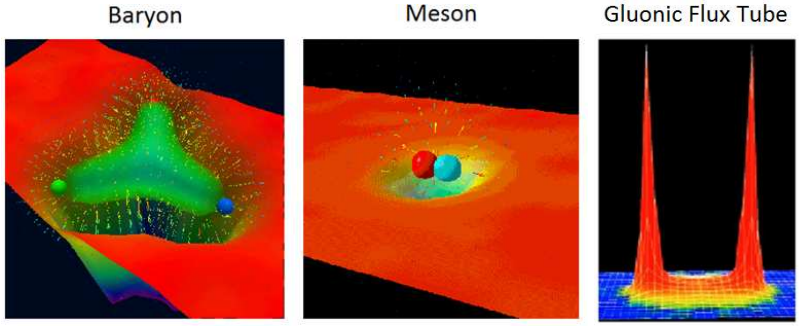

Fig. 1. Computer simulation of a baryon, meson, and the gluonic "flux tube" that forms between the quarks and anti-quarks in these hadrons. [1] [2]

But why do gluons confine quarks within the hadron? The understanding of the properties of such a strong bond still remains unknown and open for exploration. Flux-tube theory designates the hold that gluons have on quarks as a tube of chromoelectric field [3]. The field of Quantum Chromodynamics designates such a force the "Color Force", further explaining that quarks and gluons carry a "color charge" (Red, Blue, Green, AntiRed, AntiBlue, or AntiGreen). Despite nomenclature, color charge does not have optical or electrical properties. Rather, it is a way of explaining the interactions of quarks. A baryon is made of three color charged quarks: one red, one blue, and one green. A meson is composed of a quark and an antiquark: color and anti-color. In both cases, the total color is white. Although quarks are constantly changing color as gluons transfer new charges, the net-color of any hadron is colorless. As we pull apart a quark and an anti-quark and stretch this color force, it only grows stronger, making it heretofore impossible to isolate a single color [1].

Quantum Chromodynamics has successfully mapped several mesons outside of the standard quark model, yet there appears to be evidence of another "exotic" state [4]. These exotic mesons exhibit J^{PC} (where J is spin, P is parity, and C-parity) quan-

tum numbers that are not possible in the $q\bar{q}$ model [5]. Mesons in which the glue is excited form hybrid mesons ($q\bar{q}g$), some of which have these exotic qualities. By mapping out the spectrum of the exotic hybrid mesons produced by excitation of the gluonic field binding quarks, it is hoped that confinement can be better understood.

1.2 GlueX

GlueX is a high energy quantum chromodynamics experiment located in Hall D at Jefferson Lab (JLab), Virginia. The goal of the experiment is to collect the data necessary to understand the confinement of quarks by mapping the spectrum of the exotic hybrid meson. Hybrid mesons, with their high degrees of gluonic freedom, serve as an ideal probe into the gluonic field, and thus are a central aspect of the experiment. GlueX makes use of a process called "photoproduction", in which a photon is excited to act as a virtual vector meson [6]. This meson, when incident on a proton, produces a vast array of new particles, including some exotic hybrid mesons. In order to produce a photon beam, the experiment begins by running a stream of electrons through an underground accelerator until it reaches 12 GeV. Such an energy is required as the desired range of particle (mesons, glueballs, and exotic hybrid mesons) mass is 3 GeV/c^2 [4].

The electron beam then travels into Hall D where it is focused onto a thin diamond wafer. Angled correctly, this diamond causes coherent bremsstrahlung radiation, meaning that some of the electrons emit gamma rays (photons). This 9 GeV linearly polarized photon beam continues through a vacuum into the solenoid detector where it collides with the protons in a liquid hydrogen target. Here, energy is converted into mass, and a vast array of new particles (mostly hadrons) is created [3]. Various detectors work to track the decays of these particles, which can be reconstructed to better understand the properties of the exotic hybrid meson, and thus the gluonic field.

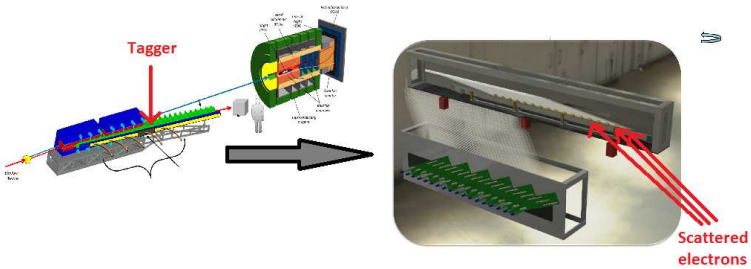

Fig.2. Depiction of the GlueX experiment with the electron beam entering from the left in the first frame. The second frame emphasizes and zooms in on the tagger microscope and the scintillating fiber array [7].

After the coherent bremsstrahlung, the main electron beam is bent by two large magnets toward the electron dump. Those electrons which emitted a photon,

however, are degraded in energy and thus have less momentum. They therefore spend more time in the magnetic field and have a larger bend radius. Bend radius then becomes an indication of momentum, allowing the tagger microscope to separate electrons by their energy. These degraded electrons pass through a short vacuum before striking the spectrometer and passing through an aluminized Mylar window into an array of scintillating optical fibers, seen in Figure 2 [4]. The fibers are 2mmx2mm in their cross section, and are arranged in bundles five high and three wide. Each bundle represents an 8 MeV energy increment [8]. The electrons strike the scintillating fibers and travel through them, creating a flash of light as they do. This signal is then transmitted by a regular optical fiber to a silicon photomultiplier light sensor (SiPM) which detects an electron of that certain energy. A signal is then sent to the main detector, "tagging" this energy to the incoming photon. Because of the wide range of energy (around 4 MeV) allowed to detect electrons, we are able to accurately tag the photon with high certainty, safe from violating Heisenberg's Uncertainty Principle by several orders of magnitude [9]. Knowing the initial energy of the photon is essential in reconstructing the exotic hybrid mesons.

1.3 Scientific Goals: Calibration Device

The prime goal of GlueX's team at the University of Connecticut is to properly tag the photon's initial energy with the tagger microscope. But how do we ensure that this data is accurate? In order to explore a particle state that has never been observed, it is essential that the scintillating fibers are functioning properly and transducing signals correctly. My goal was to design and build a calibration device for the scintillating fibers of the tagger microscope. As detailed in this paper, the device will rest above the tagger microscope and move remotely back and forth such that it is able to deliver light pulses to the fiber bundles. Various tests were done to ensure that this method could properly simulate the passing of electrons through the fibers. A mechanized calibration device is a seemingly small – but nonetheless critical – element of the GlueX experiment.

2 Methodologies

2.1 Mechanical Set-Up

While the GlueX experiment is running, access to Hall D will be restricted for days at a time. Nonetheless, it is imperative to the accuracy of the data collected that the scintillating fibers are functioning correctly. It is therefore essential to have a built in framework for a calibration device that can be controlled remotely from out-

side of the building. The framework should be about a meter long such that the device can reach all of the fiber bundles, it should be relatively fast, and it should be accurate.

The final design selected was a one-meter long ridged aluminum beam that would act as a track for a sliding cart upon which a laser diode was connected. Two flanged timing pulleys at either end of the metal track are connected by a timing belt, both ends of which are connected to the cart. The belt is driven by a Lin-Engineering 1.8 degree stepper motor, which in turn is commanded by a computer program. The cart will slide in above the tagger on the fiber side of the Mylar window.

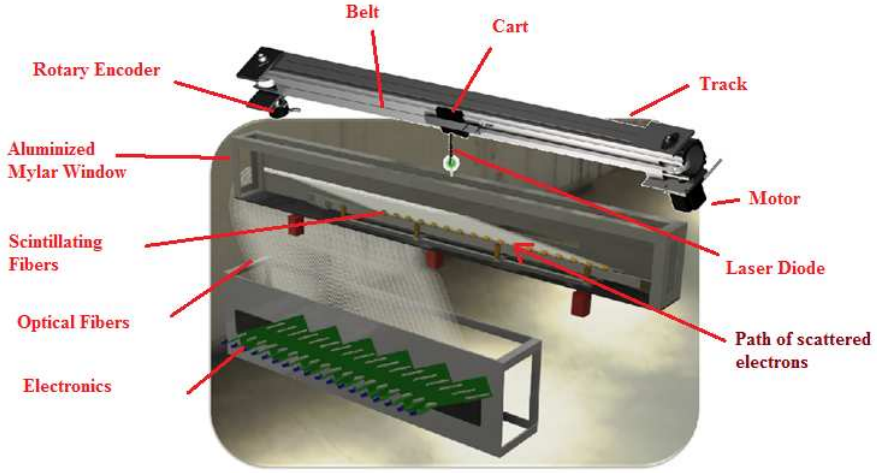

Fig.3. Calibration device design superimposed with the tagger microscope [7].

The maximum deflection of the beam was determined to be 6um [10] or negligible. By placing the timing pulleys just slightly above the top of the beam, the belt will be pulling the cart with maximum tension and control. The right side of the beam, as in accordance with Figure 3, consists of the 1.8 degree "WO-5718X-05E" Lin-Engineering Stepper Motor, secured into place with a piece of aluminum such that the turning axel extends through a drilled hole into the side of the beam. A 0.25" inner diameter coupling was used to extend the motor's axel with a 0.25" shaft. On this shaft rests the 1.783" diameter flanged timing pulley. The other end of the shaft extends through a hole on the opposite side of the beam and rests in a 0.25" bearing. On the left side of the beam, there is a similar set up. A 1.783" diameter flanged timing pulley with a 0.375" bore is held in place by a 0.375" diameter shaft, which rests in two bearings on either side of the beam. The shaft continues to extend out a couple inches past the bearing such that a rotary encoder can be secured – the inside of this encoder will turn in step with the pulley. A 0.375" diameter belt extends over both pulleys and connects to the cart with two light folding aluminum pieces. All parts were purchased from SDP-SI. A laser diode will be secured to the top of the cart, and the entire framework will be inverted for implementation so the laser diode can hover above the fiber bundles. All machining of parts was performed by Brendan Pratt, a graduate student Dr. Jones' Nuclear Physics Lab, UConn.

2.2 Electronics

In order to control the motor adequately, a LabVIEW program was written that communicates with a Digital to Analog Controller (DAC) via USB (see Figure 4). Connected by various wires to this DAC is a R208 microstep driver. The LabVIEW program opens and closes the various circuits to move the cart back and forth. The 5V logic power of the driver is connected to the 5V output on the DAC, while the 24V driver power wire is connected to ground on the power supply.

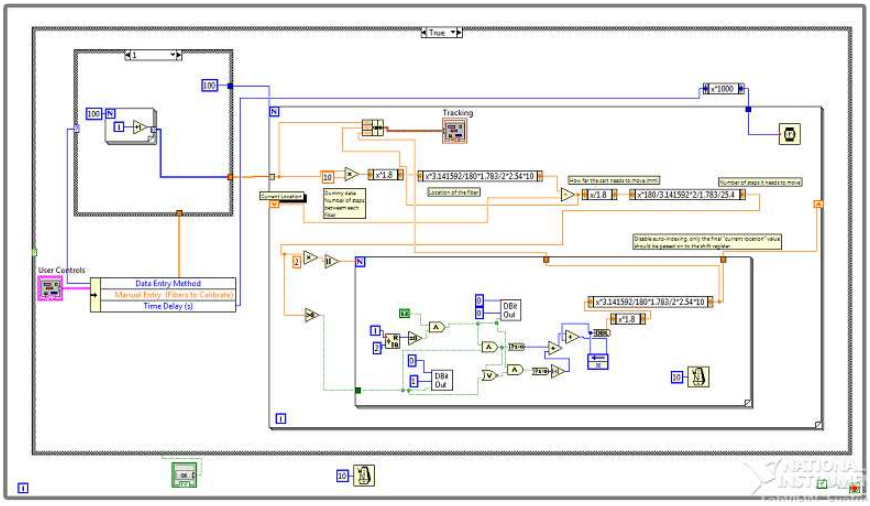

Fig.4. Screen-shot of block diagram of LabVIEW program that controls the motor.

The program was written to be user driven. A user inputs a series of fibers to be calibrated, and the robot travels to those fiber bundles flashing light pulses to calibrate them. For convenience, quick calibration options were built in such as 'all', 'odd', 'even', 'manual', and 'reset'. The reset button moves the cart from its current location back to zero. The interface allows the user to track the location of the cart.

2.3 Light Distribution

The prime purpose of the calibration device is to simulate the axial movement of scattered electrons through an array of optical fibers in the tagger microscope. With the passing of each high energy electron, the fibers "scintillate", sending a signal via waveguide to Silicon Photomultiplier light detectors [3]. In this way, the presence of electrons – and thus photons – of various energies can be detected. Such a phenomenon can be simulated with a low energy green laser diode to test the functionality of the optical fibers. The light, rather than the electrons, will traverse the fibers. Two methods were explored for light distribution: (1) Wave-shifting fibers, and (2) Mylar beam reflection. See Figure 5 for visual representation.

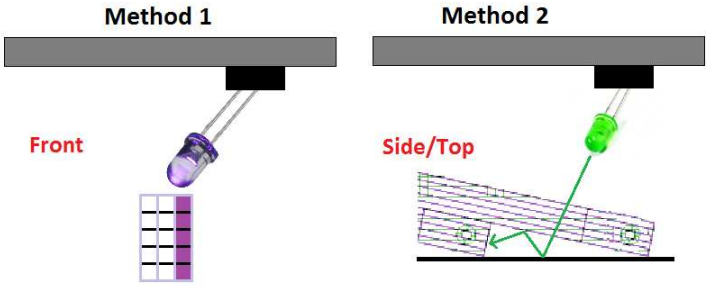

Fig.5. The two disputed methods for light distribution: wavelength-shifting fibers and mylar beam reflection.

2.3.1 Wavelength-shifting Fibers

Just as the scintillating fibers glow bright when electrons pass through them, wavelength-shifting fibers illuminate when UV light passes through them. If these fibers were lined parallel to the focal plane of the scintillating fibers such that each wave-shifting fiber covered one column of scintillating fibers, then light could easily and effectively be distributed to the scintillating fibers. The laser would simply hover over the fiber bundle and pass from column to column releasing short pulses of UV light. During the real-time experiment, the scattered electrons would be moving so fast that the wave-shifting fibers would not act as a barrier or significantly alter the electron energies. While wave-shifting fibers have proven to be effective, the installation would be costly and time consuming. Thus before further examining this option, the section method was taken into account.

2.3.2 Mylar Beam Reflection

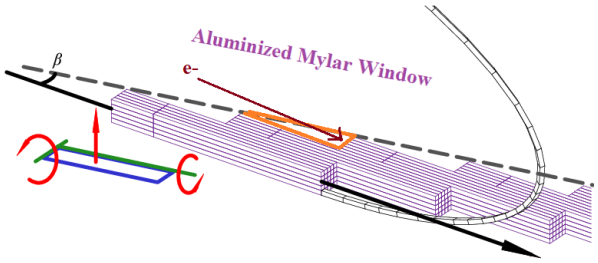

Fig.6. The optical fiber array viewed from behind, with the reflective triangular prism highlighted in orange. Electrons will be entering through the window [7].

Post-bremsstrahlung degraded electrons are bent by a magnetic field in a radial spread corresponding to momentum [11]. These electrons pass through a short vacuum before striking the spectrometer's focal plane and passing through a thin aluminized Mylar window to the optical fiber array. The fiber bundles are arranged flesh

with this Mylar window, skewed at an angle of β= 11.9 degrees as seen in Figure 6. This creates a triangular prism between each bundle's focal plane, its neighboring bundle's edge, and the aluminized Mylar window. The scintillating fibers are coated in Mylar as well, creating a prism optimal for light reflection. It was hypothesized that a laser diode positioned correctly above the prism could effectively distribute light to the fibers. Such a theory was tested via a Monte Carlo Matlab simulation.

Given various inputs, the program was built to display a model of the laser diode beam interacting with the reflective prism and to calculate the percent and spread of light transduced by the optical fibers. One of the first tasks was thus constructing the laser beam. The project was begun under the initial assumption that the beam would follow Gaussian randomizations and would obey the single-slit diffraction limit. The focal plane of the beam was set in the zy-plane, meaning that Gaussian distributions would be necessary in both of these directions to determine each photon's origin. Likewise, separate distributions would define each photon's angle.

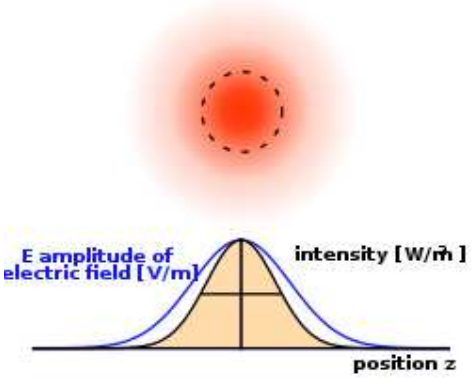

Fig.7. A depiction of gaussian spread: how intensity of the beam varies with position (z). [12]

The spot-size, shown in Figure 7, of the laser was left as a variable in the program considering that it depends on laser type. Initially, it was defined as:

$$\Delta z = 2 * 10^{-6} \text{ meters r.m.s} \quad \textbf{(1)}$$

$$\Delta y = 2 * 10^{-6} \text{ meters r.m.s.} \quad \textbf{(2)}$$

From these standard deviations, the radial spread was calculated. The Heisenberg Uncertainty Principle gives a relation between spread in position and momentum:

$$\Delta x \Delta p = \frac{\hbar}{2} \quad \textbf{(3)}$$

Knowing also the general relationship between momentum and wavelength, and that the change in momentum of a scattered photon will be its change in angle divided by its momentum, the above equation can be reduced. The "h" is Plank's Constant: $6.626 * 10^{-34} \frac{m^2 kg}{s}$.

$$p = \frac{h}{\lambda} \quad , \quad \Delta p = \frac{\Delta\theta}{p} \tag{4, 5}$$

$$\Delta p = \frac{\hbar}{2\Delta x} = \frac{\Delta\theta}{p} \tag{6}$$

$$\Delta\theta = \frac{\hbar p}{2\Delta x} = \frac{\hbar h}{2\Delta x \lambda} = \frac{\lambda}{4\pi\Delta x} \tag{7}$$

Since a green laser diode was being modeled, the wavelength (λ) was assumed to be 532 nm. Substituting the z and y Gaussian distributions in the above single-slit diffraction limit yielded that radial spread in the z and y directions [13]. When this yielded a dispersion of only about 1.2 degrees, it was decided that a single-slit diffraction governed laser was not correct. The typical laser diode has a much wider spread. Thus for the model, the following typical values in Table 1 were assumed for development (subject to change upon purchase of the laser):

Table 1. Set variables assumed for the Gaussian randomization for the purpose of modeling.

Gaussian Variable	Value
Δz	$100*10^{-6}$ meters
Δy	$1*10^{-6}$ meters
$\Delta\theta_z$	$8*(\frac{\pi}{180})$ radians
$\Delta\theta_y$	$40*(\frac{\pi}{180})$ radians

Given an initial width separation of the laser from the bundle along the x-axis and the angle phi (drawn from the positive x-axis to the positive z-axis) as inputs, the program was written to calculate the optimum origin for the laser such that the center of the beam strikes the center of the bundle. From this initial location, the Gaussian spread was created using Matlab's "`normrnd(mu,sigma)`" function. This function gives a random number from a normal (Gaussian) spread centered at mu, with a standard deviation of sigma.

After defining the respective origins of the photons, each photon was tracked separately through an extensive series of loops, directed by its angle values. Each photon bounced in the prism in accordance with Snell's Law [14]:

$$\theta_{incident} = \theta_{reflected} \tag{8}$$

However on average, Mylar with refractive index 1.65 only reflects 94% of light [15]. Therefore, every time a photon bounces, it is modeled almost as a wave in that it loses 6% of its light content. Additionally when a photon strikes the fiber bundle, of the 6% light not reflected only a small portion actually enters each fiber. This is

due to the fiber's angle of acceptance and refraction. The optical fibers transmit light via total internal reflection, meaning that light has to strike the fiber at an angle of $\pm 35.7^{\circ}$ in order to confine the light properly [16]. In addition, only a small portion of the light is refracted. The percent of light from each wave-like photon that passes through each fiber was calculated with Fresnel's Equations [17]. As the photon bounces through the prism, it is governed by two ever-changing vectors: $\hat{k}$ and $\hat{e}$. $\hat{k}$ is the unit vector describing the motion of the photon itself, and $\hat{e}$ is the unit vector describing the electric field. The main laser beam is defined to be linearly polarized with the electric field perpendicular to the beam and oriented at 0 degrees for simplicity. The normal ($\hat{n}$) to the fiber bundle's focal plane is equal to [0 1 0], as this plane is the xz-plane.

To determine the amount of light refracted, the incident light must be split into the two different polarizations of which it is composed: s (where the electromagnetic field is in the focal plane of the bundle) and p (where the electromagnetic field is perpendicular to the plane of the bundle). This is done by crossing the vectors to get $\hat{k}$'s components, and then dotting these components with $\hat{e}$ to get $\hat{e}$'s components.

$$\hat{s} = \frac{<\hat{n} \times \hat{k}>}{|\hat{n} \times \hat{k}|} \quad , \quad \hat{p} = \frac{<\hat{k} \times \hat{s}>}{|\hat{k} \times \hat{s}|} \qquad \textbf{(9, 10)}$$

$$e_s = \hat{e} \cdot \hat{s} \quad , \quad e_p = \hat{e} \cdot \hat{p} \qquad \textbf{(11, 12)}$$

Using the definition of a dot product, the incident angle of the light on the surface can be calculated:

$$\theta_i = cos^{-1}(|\hat{n} \cdot \hat{k}|) \qquad \textbf{(13)}$$

The refractive index of air used is the standard, 1.0003 [15]. Because the light is travelling from air to Mylar, the first refractive index is air (n_1= 1.0003) and the second refractive index is Mylar (n_2 = 1.65). Fresnel's equations then provide the reflectivity due to s and p polarization respectively [17]:

$$R_s = \left| \frac{n_1 cos\theta_i - n_2 \sqrt{1 - \left(\frac{n_1}{n_2} sin\theta_i\right)^2}}{n_1 cos\theta_i + n_2 \sqrt{1 - \left(\frac{n_1}{n_2} sin\theta_i\right)^2}} \right|^2 \qquad \textbf{(14)}$$

$$R_p = \left| \frac{n_1 \sqrt{1 - \left(\frac{n_1}{n_2} sin\theta_i\right)^2} - n_2 cos\theta_i}{n_1 \sqrt{1 - \left(\frac{n_1}{n_2} sin\theta_i\right)^2} - n_2 cos\theta_i} \right|^2 \qquad \textbf{(15)}$$

These two reflection constants were consolidated into a single value by finding their individual projections:

$$R_{es} = R_s * (e_s)^2 \quad , \quad R_{ep} = R_p * (e_p)^2 \qquad \textbf{(16, 17)}$$

$$R = \sqrt{(R_{ss})^2 + (R_{sp})^2} \tag{18}$$

$$T = 1 - R \tag{19}$$

Here R is the amount reflected and T is the amount transduced. The program runs until the percent of the remaining bouncing light is less than the threshold (default = 1%). The total collected light is reported as a percent of the original. The goal set was to successfully capture about 1% of the light, and to distribute it evenly amongst the fibers. “Evenly” was aimed to be on the order of 5, but no greater than the 10.

3 Results and Discussion

The calibration device was built, simulated, and tested until it was concluded that it would be an effective means for calibrating the scintillating fibers of the tagger microscope.

3.1 Mechanical and Electronic

The mechanical device is fully functional, capable of moving to different fiber locations as designated by the user. It follows the exact design proposed, and with a mounted laser will be ready for calibrating the tagger microscope. The laser will be mounted according to the results in “Light Distribution”. The robot is driven by the previously mentioned LabVIEW program which communicates to a DAC, R208 microstep driver, and stepper motor in turn. The final product can be seen in Figure 8.

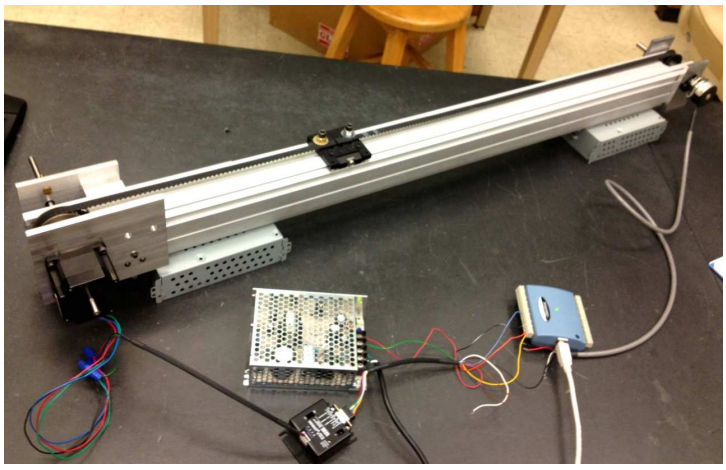

Fig.8. Final set-up of calibration device, fully functional.

3.2 Monte Carlo Program for Light Distribution

The Monte Carlo Matlab simulation was run multiple times, varying the following parameters until the results were consistently in the desired range: separated width (sepwidth), separated height (sepheight), separated length (seplength), and number of photons (numphotons). While the program optimizes the beam to strike in the center of the fiber bundle, minor adjustments needed to be made until the light was distributed evenly. The goal was to capture at least 1% of the light effectively in the fibers, and to have the amount of light captured by each individual fiber vary by no more than a factor of 10, preferably as low as 5. The fibers will be referenced by number in accordance with the following array, viewed from behind the fiber bundle's focal plane:

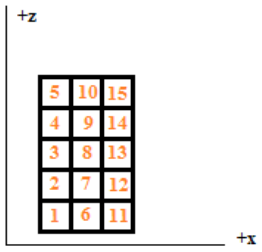

Fig.9. Array of fibers, refernced by number.

Run for 10 photons, the following Figure 10 is a visual of the simulation viewed from the side and the top. The origin of the beam is the white asterisk.

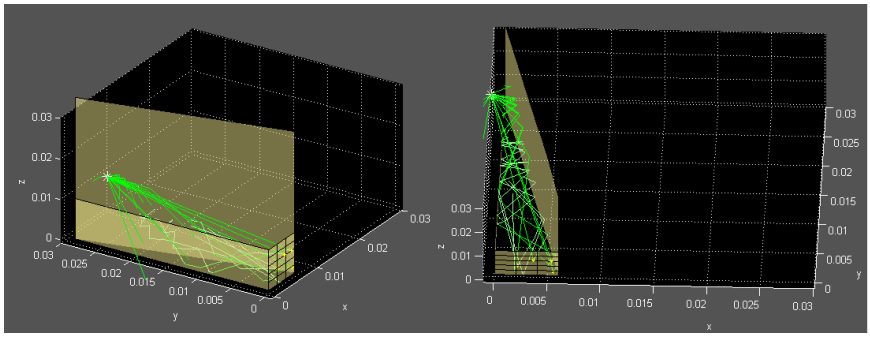

Fig.10. Example views of simulation, run for 10 photons.

In order to properly simulate a real beam, the program had to be run for at least 1,000 photons. The parameters which consistently produced results in the correct range were:

```
sepwidth = 0.001
seplength = (optimized length) – 0.00045
```

```
sepheight = (optimized height) – 0.0028
numphotons = 1,000
```

Where the optimized length is:

```
0.003*tan(78.1*pi/180)+0.003*tan(66.2*pi/180)+sepwidth*
tan(66.2*pi/180);
```

And the optimized height is:

```
tan(phiorig_rad)*(sqrt((length2^2)+(0.003^2))+sqrt((lengt
h3^2)+(sepwidth^2)-0.005+length1*tan(phiorig_rad);
```

Because this program depends on Gaussian randomization, the results will be slightly different every time. However these are the results from one of the trials with 1,000 photons run.

Table 2. Amount of light collected by each fiber, a portion of numphotons.

Fiber	Value
1	0.2672
2	1.0308
3	1.0424
4	0.8106
5	0.6572
6	0.3789
7	1.0404
8	1.3369
9	0.5041
10	0.2722
11	0.2292
12	1.0199
13	1.0552
14	0.6706
15	0.3303

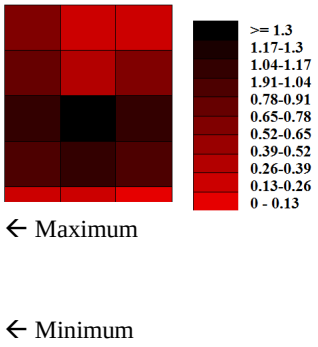

Fig.11. Array of fibers colored by amount of light absorbed.

The percent of the laser's original light that was accepted by the fibers was 1.0646%. This value is above 1%, and therefore favorable. Every time the program was run for these parameters, the percent of light captured was in this range by ±0.1%. The maximum ratio of the amounts of light collected by any two respective fibers is found by dividing the maximum value by the minimum value. Such values are

displayed in Table 2, where the fiber numbers correspond to the diagram in Fiber 9. Likewise, Figure 11 shows a color-density plot of the amount of light absorbed by each fiber. In this case, max(fiberbundle)/min(fiberbundle) = 5.833. This value is well within our limits of acceptance (<10), and extremely close to our optimal value (5). Running the program multiple times with these parameters, it became apparent that this value bounced between 5 and 6. The program generated a visual of the beam striking from these angles, as seen below. Yellow *'s represent photons which were captured by a fiber.

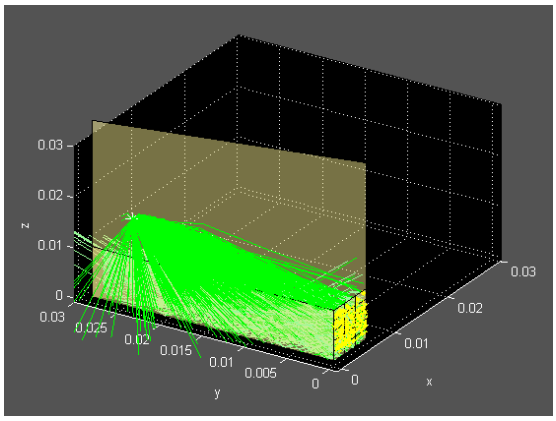

Fig.12. Simulation of laser with 1,000 photons using the final selected parameters.

From these results, one can conclude that Mylar light reflection is a reasonable and accurate method for calibrating the scintillating fibers, assuming that the laser is positioned and angled adequately. This Monte Carlo Matlab program will continue to be of use for positioning the laser for calibration. While this model is quite complex, it doesn't take into account a few factors, such as the separate refraction indices for the thin aluminum coating. The program also neglects interference of light waves, and is incapable of generating enough photons to accurately simulate a laser beam. Nonetheless, it is precise enough to demonstrate that this method of calibration will work.

4 Conclusion

The GlueX experiment, if successful, would be the first to observe exotic hybrid mesons [11]. In addition, the data collected in the first two years is expected to exceed current photoproduction data by several orders of magnitude [6]. In this way (among others), the experiment is expected to be truly monumental – specifically by seeking to answer one of the long asked questions in physics: "Why are quarks and gluons confined inside the hadron?" When treading such novel territory, it is essential that the data collected is accurate. When reconstructing the exotic hybrid meson de-

cays in the solenoid detector, an essential piece of information is the photon's initial energy, which will be tagged by the tagger microscope. It is therefore highly important that the scintillating fibers of the tagger microscope are functioning correctly, and accurately transducing signals representing the momenta of the electrons. The calibration device proposed and built is believed to solve this problem. An aluminum ridged track on which a laser-diode cart is driven by a LabVIEW controlled stepper motor, the device simulates the passing of scattered electrons by bouncing light into the fibers. Using the aluminized Mylar window and the Mylar coated fibers as a reflective prism, the beam is bounced from above into the fiber bundle into the fibers. The light causes the fibers to scintillate in a similar manner as the high-energy electrons do. A Monte Carlo Matlab program proves that at least one percent of the light from the laser diode could be captured in this manner, and that no fiber would accept an amount of light more than ten times greater than another (usually around five times). This program models the laser diode as a Gaussian beam, and uses Fresnel's equations to ensure proper reflective and refractive properties. While a relatively small aspect of the GlueX experiment, a calibration device for the scintillating fibers of the tagger microscope will be one of many important methods of ensuring experimental accuracy.

5 Future Work

Both the LabVIEW and Matlab programs were soft-coded such that they may be changed at any point to reflect alterations in the experiment. For example, if the distance between fiber bundles is changed, the LabVIEW program can be quickly altered to direct the cart to new locations. If the type of laser is changed, the Gaussian spread can likewise be changed in the Matlab program to accurately model a new laser. The Matlab program can also be improved by adding in aluminum refraction and running it for more photons[1]. Improvements can still be made to the calibration device; for instance, a pressure sensor at the end of beam to ensure that the reset button doesn't try to bring the cart too far back. Also, the device currently moves relatively slowly, and the device could be improved to support a faster paced calibration. In terms of the general experiment, GlueX is opening the door to an entirely new realm of scientific exploration. If this incredibly strong qluonic bond can be understood, perhaps it can be harnessed. If we can understand the potential energy stored in the gluonic bonds linking anti-quarks, then the understanding of anti-matter is close in sight. Physics is constantly building on itself, each step allowing for others to be taken. If GlueX is successful in understanding the confinement of quarks and gluons within the hadron, opportunities won't expand simply in quantum chromodynamics, but in other fields of physics and energy as well. In essence, the future work of this calibration device may be relatively short-sighted, but that of this experiment as a whole is infinite.

[1] For access to source code, email emily.briere@duke.edu

6 Acknowledgments

Thank you to the National Science Foundation for the opportunity to conduct this research under grant OCI-1156837, and to the head of our REU Professor Chun-Hsi Huang. Both my research mentor, Dr. Richard Jones, and my REU mentor, Dr. Heather Read, were instrumental in making this program a great learning experience. Thanks also to the graduate students in Dr. Jones' lab, who were always available to provide advice. Particular thanks are given to Brendan Pratt who machined the parts for the calibration device. Lastly, thanks to Sanka Piyadasa and John Turner for their prior work on the project.

References

1. "The Particle Adventure." *The Particle Adventure*. NSF & DOW, n.d. Web. 1 July 2012. <http://www.particleadventure.org/>.
2. Leinweber, Derek. "Visualizations of Quantum Chromodynamics." *Derek Leinweber*. Centre for the Subatomic Structure of Matter (CSSM) and Department of Physics, University of Adelaide, 2003. Web. 1 July 2012. <http://www.physics.adelaide.edu.au/theory/staff/leinweber/VisualQCD/Nobel/>.
3. Underwood, Michael "Woody" "Design of Electronics for a High-Energy Photon Tagger for the GlueX Experiment." Thesis. University of Connecticut, 2008. Print.
4. GlueX Colaboration. *A Search for QCD Exotics Using a Beam of Photons*. Rep. Vol. 4. N.p.: n.p., 2002. Print.
5. Barnes, T. *Exotic Mesons, Theory and Experiment* *. Rep. Cracow: n.p., 2001. Oak Ridge National Laboratory, 27 Feb. 2001. Web. <http://www.ornl.gov/~webworks/cpr/v823/pres/110656.pdf>.
6. The GlueX Collaboration. "Physics." *The GlueX Experiment*. Jefferson Lab, n.d. Web. 1 July 2012. <http://www.gluex.org/>.
7. McIntyre, James. *Tagger Microscope: A High-Resolution Hodoscope for the Photon Beamline of the GlueX Experiment*. *The GlueX Experiment*. University of Connecticut, n.d. Web.
8. Jones, R. T. "Performance of the Hall D Tagger Microscope as a Function of Rate." *University of Connecticut* (2010): n. pag. Web. <http://zeus.phys.uconn.edu/halld/tagger/fp-microscope/rates-10-2009/rates.pdf>.
9. Senderovich, I., C. R. Nettleton, M. Underwood, and R. T. Jones. "Design and Fabrication of a Prototype Scintillating Fiber Tagger Microscope for the GlueX Experiment." *University of Connecticut* (2008): n. pag. Web. <http://zeus.phys.uconn.edu/halld/bltwghome/UConn-Jlab_contract-2007/microscope-9-2008/report-8-2008.pdf>.
10. Turner, John. "Calibration Device for Scintillators." *UConn PAN -- GlueX Wiki*. GlueX, n.d. Web. 21 May 2012. <http://zeus.phys.uconn.edu/wiki/index.php/Calibration_Device_for_Scintillators>.
11. "The GlueX Wiki." *The GlueX Wiki*. GlueX Collaboration, n.d. Web. 21 May 2012. <http://wiki.gluex.org/index.php/HOWTO_get_your_jobs_to_run_on_the_Grid>.
12. "Gaussian Beam." *Wikipedia*. Wikimedia Foundation, 25 July 2012. Web. 25 July 2012. <http://en.wikipedia.org/wiki/Gaussian_beam>.

13. "Chapter Sixteen: Optics of Gaussian Beams." *Ece.umd.edu*. N.p., n.d. Web. <http://www.ece.umd.edu/~davis/chapter16.pdf>.
14. "The Mathematics of Refraction: Snell's Law." *The Physic's Classroom*. ComPADRE, 1996. Web. 1 July 2012. <http://www.physicsclassroom.com/class/refrn/u14l2b.cfm>.
15. Wood, Robin. "Refraction Index of Various Substances for 3D Modelers." *Robinwood.com*. N.p., n.d. Web. <http://www.robinwood.com/Catalog/Technical/Gen3DTuts/Gen3DPages/RefractionIndexList.html>.
16. McIntyre, James. "A Typical Round Scintillating Fiber." Print.
17. *Fresnel's Equations for Reflection and Refraction*. Rep. Rutgers, n.d. Web. <www.physics.rutgers.edu/ugrad/389/FresnelsEqns.ppt>.